

Supporting Information

Dual-Emissive Bis(diphenylphosphino)amine Platinum Complexes: Structural, Reactivity, Photophysical and Theoretical Investigations

Mahboubeh Jamshidi^{a,b}, S. Reza Barzegar-Kiadehi^a, Mohsen Golbon Haghghi*^a, Behrouz Notash^a

^a Department of Chemistry, Shahid Beheshti University, Evin, Tehran 19839-69411, Iran

^b Institut für Physikalische und Theoretische Chemie, Universität Regensburg, Universitätsstrasse 31, D-93053 Regensburg, Germany

E-mail: m_golbon@sbu.ac.ir

Contents:	Page
General remarks, Computational Details and X-ray Structure Determination	S0-S1
Figure S1-S14. The ¹ H and ³¹ P NMR spectra of complexes 2a-d , 3a-c .	S2-S8
Figure S15. (i) ORTEP representation and (ii) π-π stacking interactions for 3b .	S9
Table S1. The crystal data and structure refinement for complexes 2a , 2c , 2d , 3a , and 3b .	S10
Table S2. Experimental absorption parameters for complexes 2 and 3 in CH ₂ Cl ₂ and benzene.	S11
Figure S16. Normalized absorption spectra of complexes 2 and 3 in CH ₂ Cl ₂ at 298 K.	S12
Figure S17. Normalized emission spectra of complexes in CH ₂ Cl ₂ (10 ⁻⁴ M) at 298 K.	S12
Figure S18. Normalized emission spectra of complexes 2 in powder form at 298 K.	S13
Figure S19. Normalized emission spectra of complexes 2 in powder form at 77 K.	S13
Figure S20. Normalized excitation and emission spectra of 3a , 3b , and 3c in PMMA at 77 K and 298 K.	S14-15
References	S16

General remarks

The microanalyses were performed using Elementar CHN elemental analyzer. The NMR spectra were recorded on a Bruker Avance DPX 300 MHz spectrometer. The operating frequencies and references, respectively, are shown in parentheses as follows: ^1H (300 MHz, TMS), ^{31}P (121 MHz, 85% H_3PO_4). The chemical shifts and coupling constants are in ppm and Hz, respectively. The UV-vis absorption spectra were recorded on a Shimadzu UV-2100 spectrophotometer in a cuvette with a 1 cm and/or 1 mm path length. Emission and excitation spectra were recorded with a Horiba Jobin Yvon Fluorolog 3 steady-state fluorescence spectrometer at 298 and 77 K. This spectrometer was modified to allow for measurements of emission decay times. A PicoQuant FB-375 pulsed diode laser ($\lambda_{\text{exc}} = 378$ nm, pulse width 100 ps) was applied as the excitation source. The emission signal was detected with a cooled photomultiplier attached to a FAST ComTec multichannel scalar card with a time resolution of 250 ps. Photoluminescence quantum yields were determined using a Hamamatsu system for absolute PL quantum yield measurements (type C9920-02) equipped with an integrating sphere with a Spectralon inner surface coating. Polymer films containing about 1 weight% of the Pt complexes were obtained by dissolving the emitter and Poly(methyl methacrylate) (PMMA) in dichloromethane and spin-coating the solutions onto quartz glass substrates. All measurements were performed under a continuous flow of nitrogen gas in order to minimize emission quenching by oxygen. The monomeric precursors $[\text{Pt}(\text{C}^\wedge\text{N})\text{Cl}(\text{DMSO})]^1$, $\text{C}^\wedge\text{N} = \text{bhq}$, **1a**; ppy, **1b**, $[\text{Pt}(\text{C}^\wedge\text{N})(\text{CF}_3\text{CO}_2)(\text{SMe}_2)]^2$, $\text{C}^\wedge\text{N} = \text{bhq}$, **1c**; ppy, **1d**, were synthesized as reported in the literature.

Computational Details

Density functional calculations were performed with the program suite Gaussian 09³ using the B3LYP level of theory. The LANL2DZ basis set⁴ was chosen to describe Pt. The 6-31G(d) basis set was used for other atoms. The geometries of complexes were fully optimized by employing the density functional theory without imposing any symmetry constraints. To evaluate and ensure the optimized structures of the molecules, frequency calculations were carried out using analytical second derivatives. In all cases only real frequencies were obtained for the optimized structures. Solvent effects have been taken into account using the PCM model^{5, 6}.

X-ray Structure Determination

The X-ray diffraction measurements were carried out on STOE IPDS-II or IPDS-2T diffractometer with graphite-monochromated Mo $\text{K}\alpha$ radiation. All single crystals were mounted on a glass fiber and used for data collection. Cell constants and an orientation matrix for data collection were obtained by a least-square refinement of the diffraction data. Diffraction data were collected in a series of ω scans in 1° oscillations and integrated using the Stoe X-AREA⁷ software package. A numerical absorption correction was applied using X-RED⁸ and X-SHAPE⁹ software. The data were corrected for Lorentz and polarizing effects. The structures were solved by direct methods¹⁰ and subsequent difference Fourier maps and then refined on F^2 by a full-matrix least-squares procedure using anisotropic displacement parameters.¹¹ Atomic factors are from the International Tables for X-ray Crystallography¹². All non-hydrogen atoms were refined with anisotropic displacement parameters. Hydrogen atoms

were placed in ideal positions and refined as riding atoms with relative isotropic displacement parameters. All refinements were performed using the XSTEP32 crystallographic software package.¹³

Atomic coordinates and displacement parameters are deposited with the Cambridge Crystallographic Data Centre. The CCDC 1964741 (**2a**), 1964742 (**2c**), 1964745 (**2d**), 1964744 (**3a**), 1964746 (**3b**), contain the supplementary crystallographic data for this paper. The crystal data of complexes **2a**, **2c**, **2d**, and **3a** are shown in Table S1.

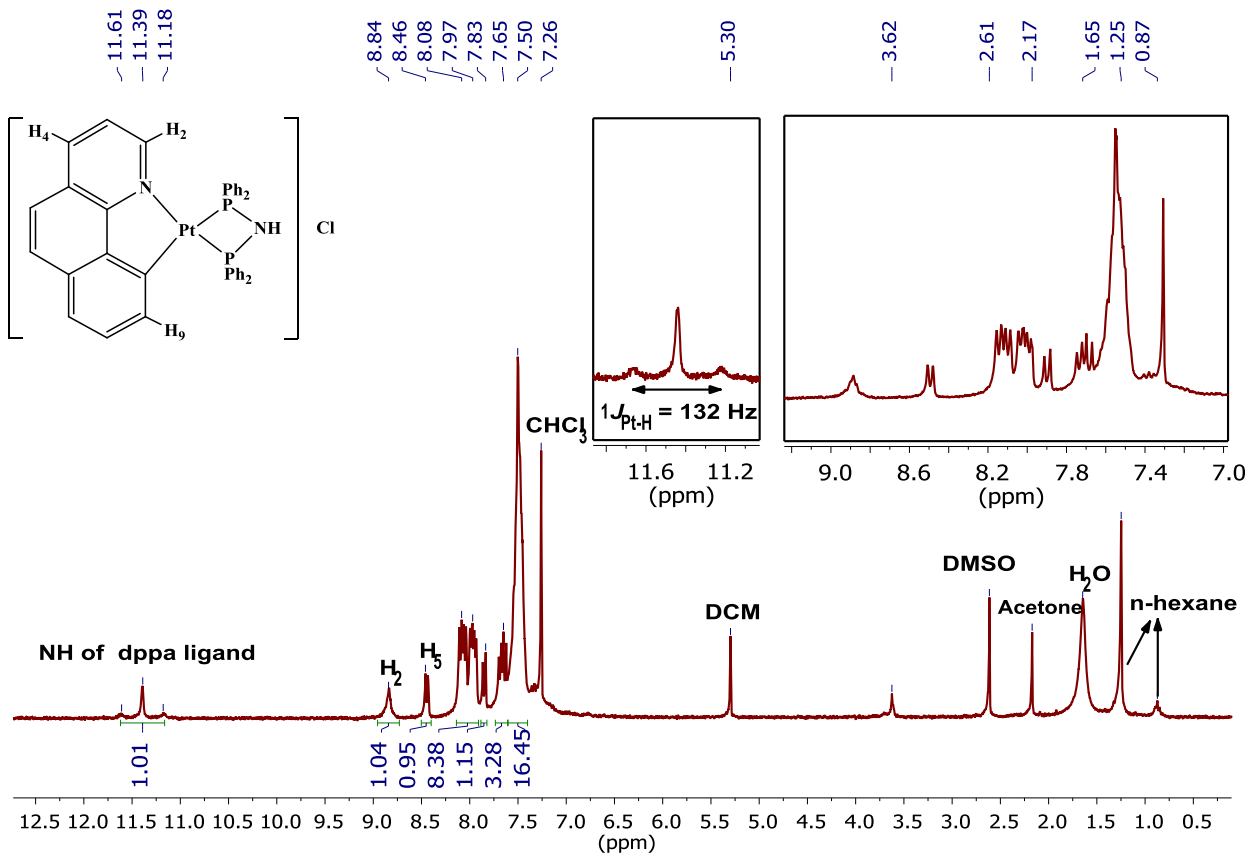


Figure S1. The ^1H NMR spectrum of $[\text{Pt}(\text{bhq})(\text{dppa})]\text{Cl}$, **2a**, in CDCl_3 .

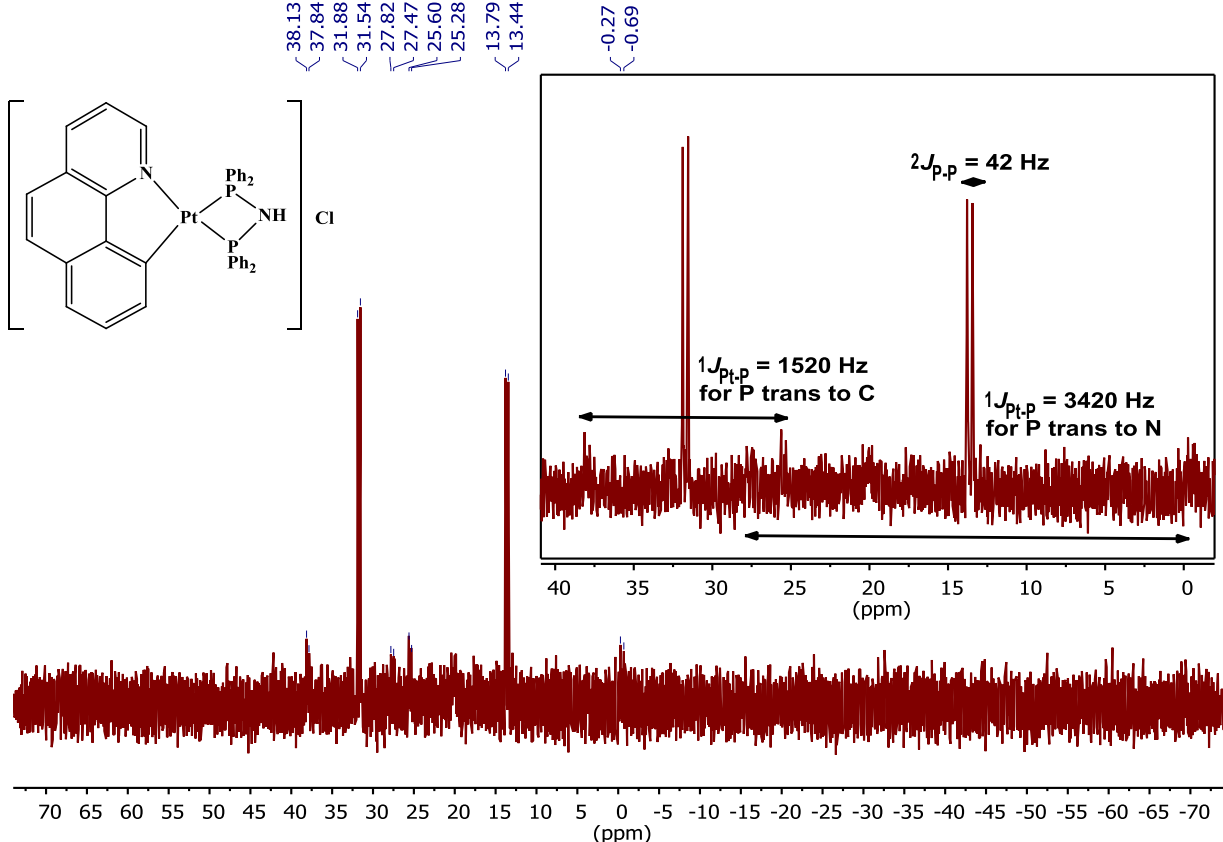


Figure S2. The ^{31}P NMR spectrum of $[\text{Pt}(\text{bhq})(\text{dppa})]\text{Cl}$, **2a**, in CDCl_3 .

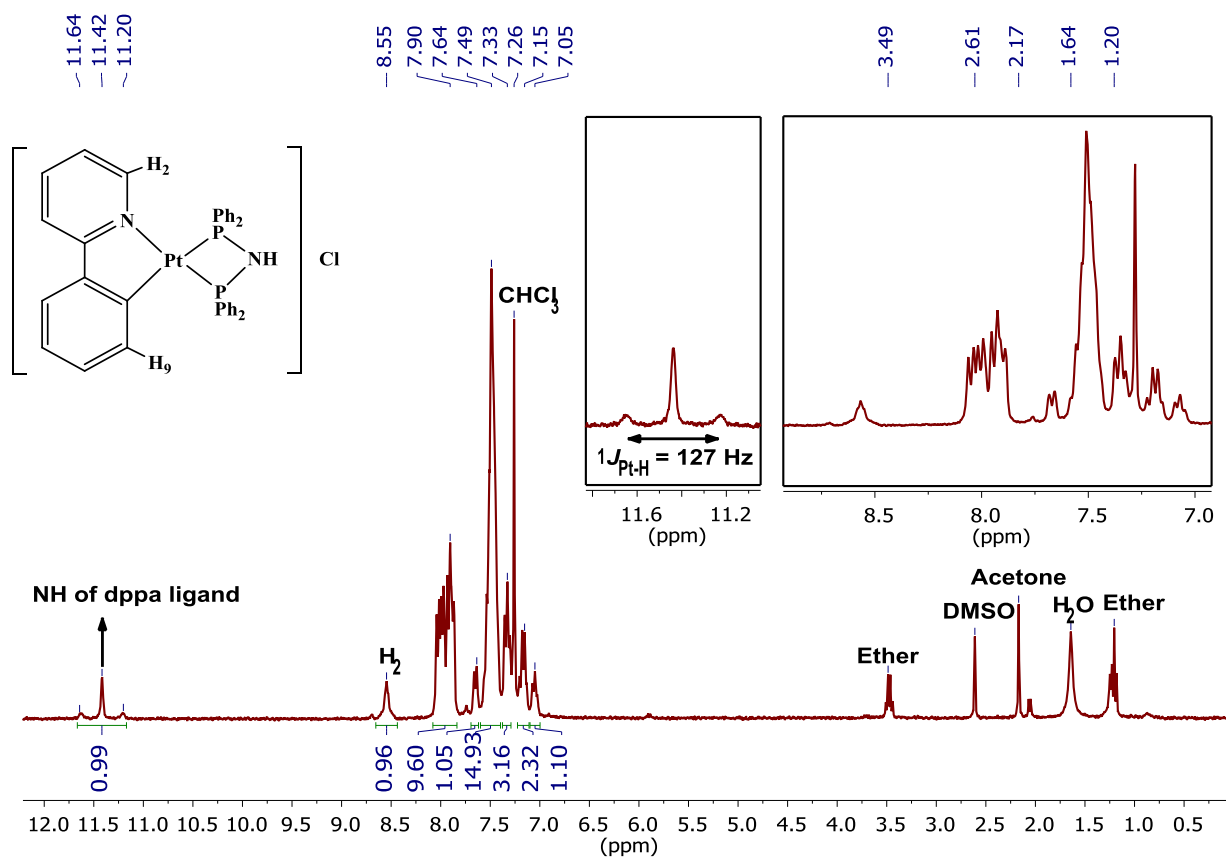


Figure S3. The ^1H NMR spectrum of $[\text{Pt}(\text{ppy})(\text{dppa})]\text{Cl}$, **2b**, in CDCl_3 .

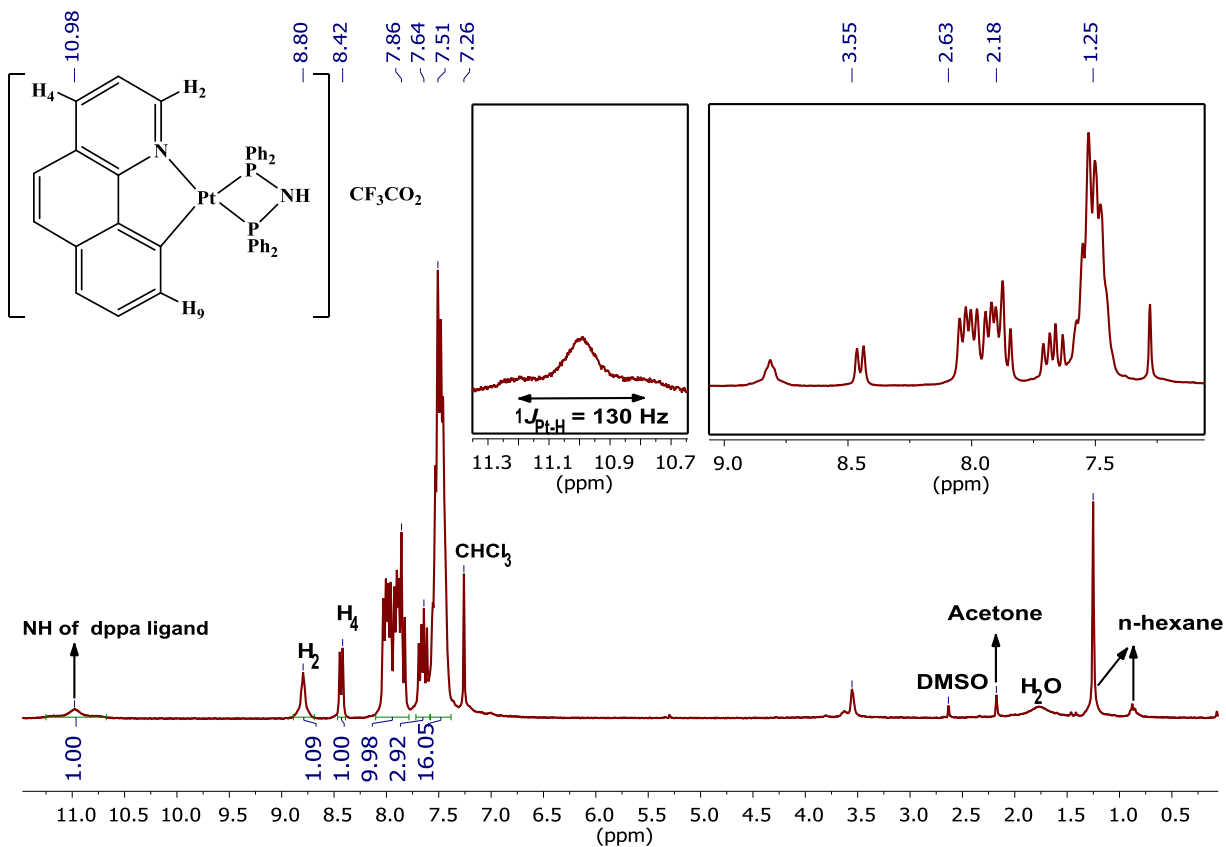


Figure S4. The ^1H NMR spectrum of $[\text{Pt}(\text{bhq})(\text{dppa})]\text{CF}_3\text{CO}_2$, **2c**, in CDCl_3 .

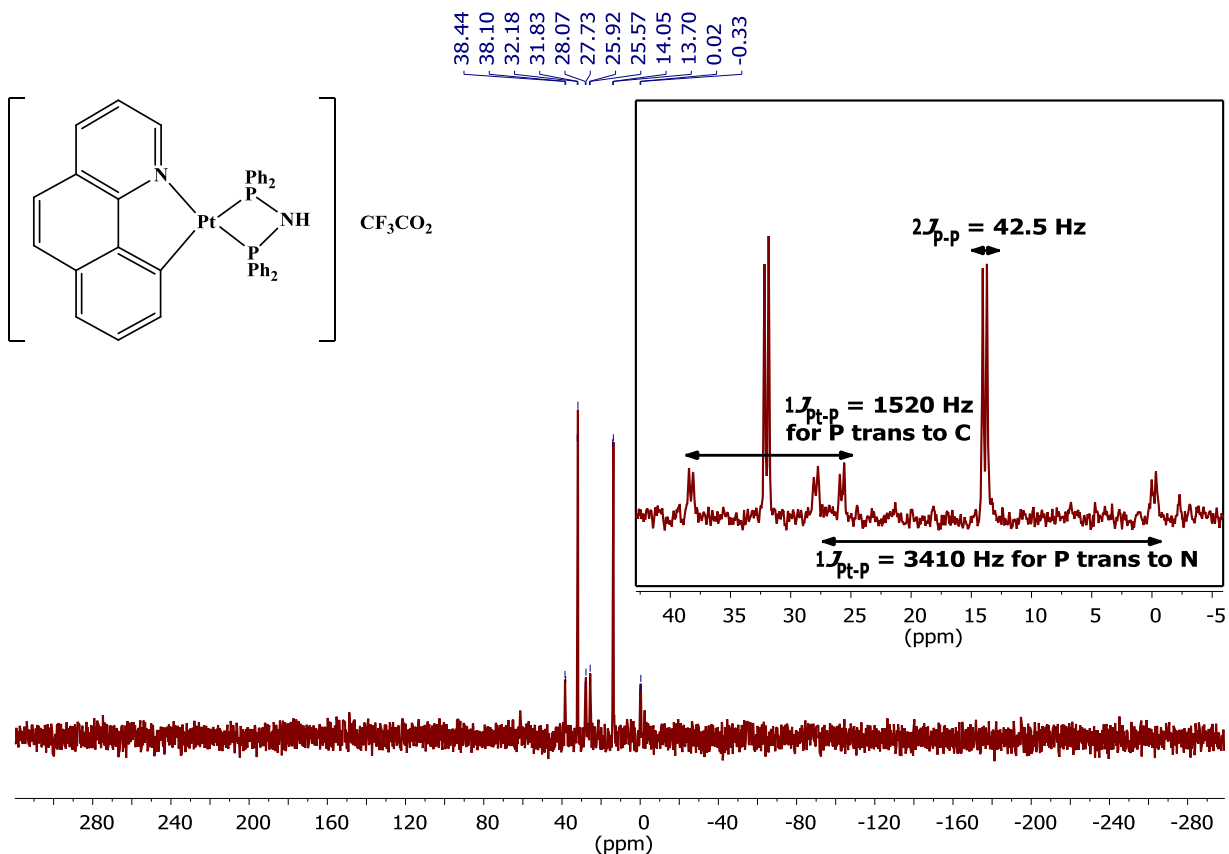


Figure S5. The ^{31}P NMR spectrum of $[\text{Pt}(\text{bhq})(\text{dppa})]\text{CF}_3\text{CO}_2$, **2c**, in CDCl_3 .

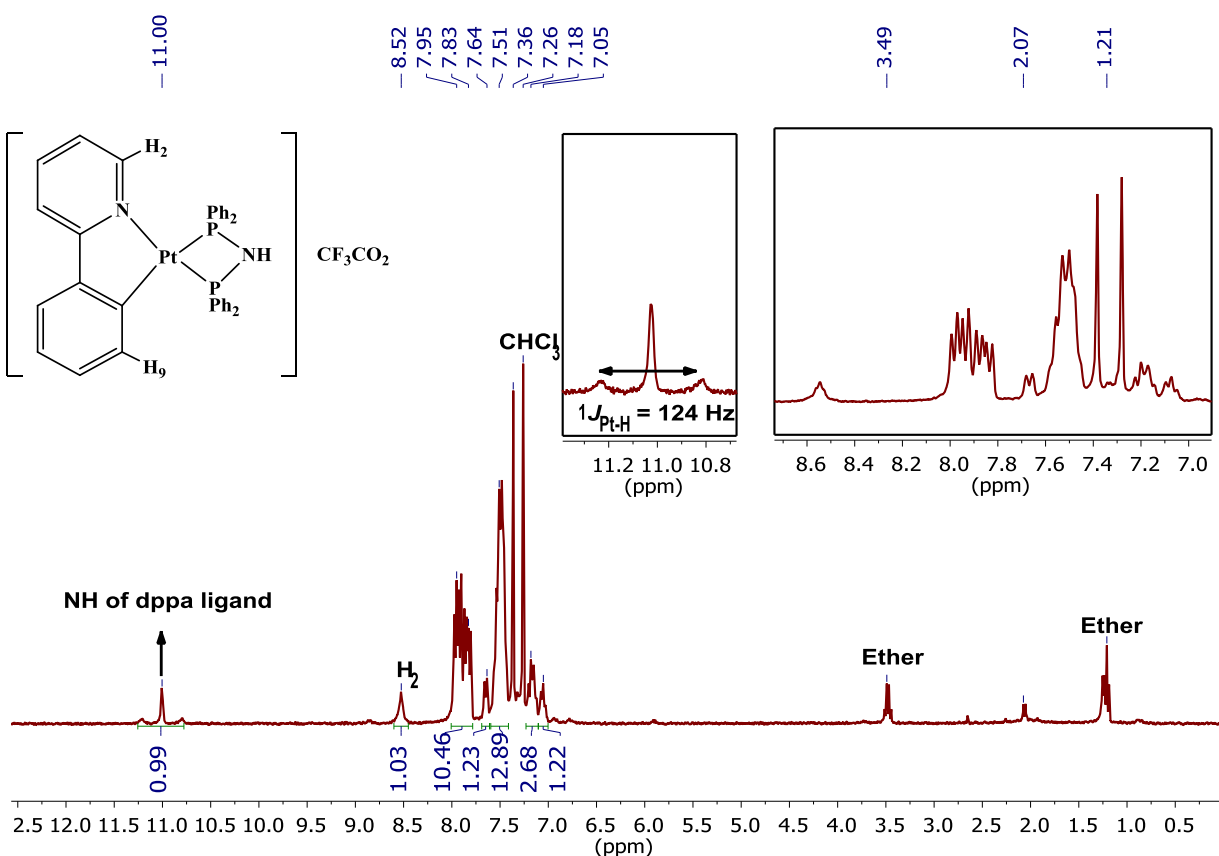


Figure S6. The ^1H NMR spectrum of $[\text{Pt}(\text{ppy})(\text{dppa})]\text{CF}_3\text{CO}_2$, **2d**, in CDCl_3 .

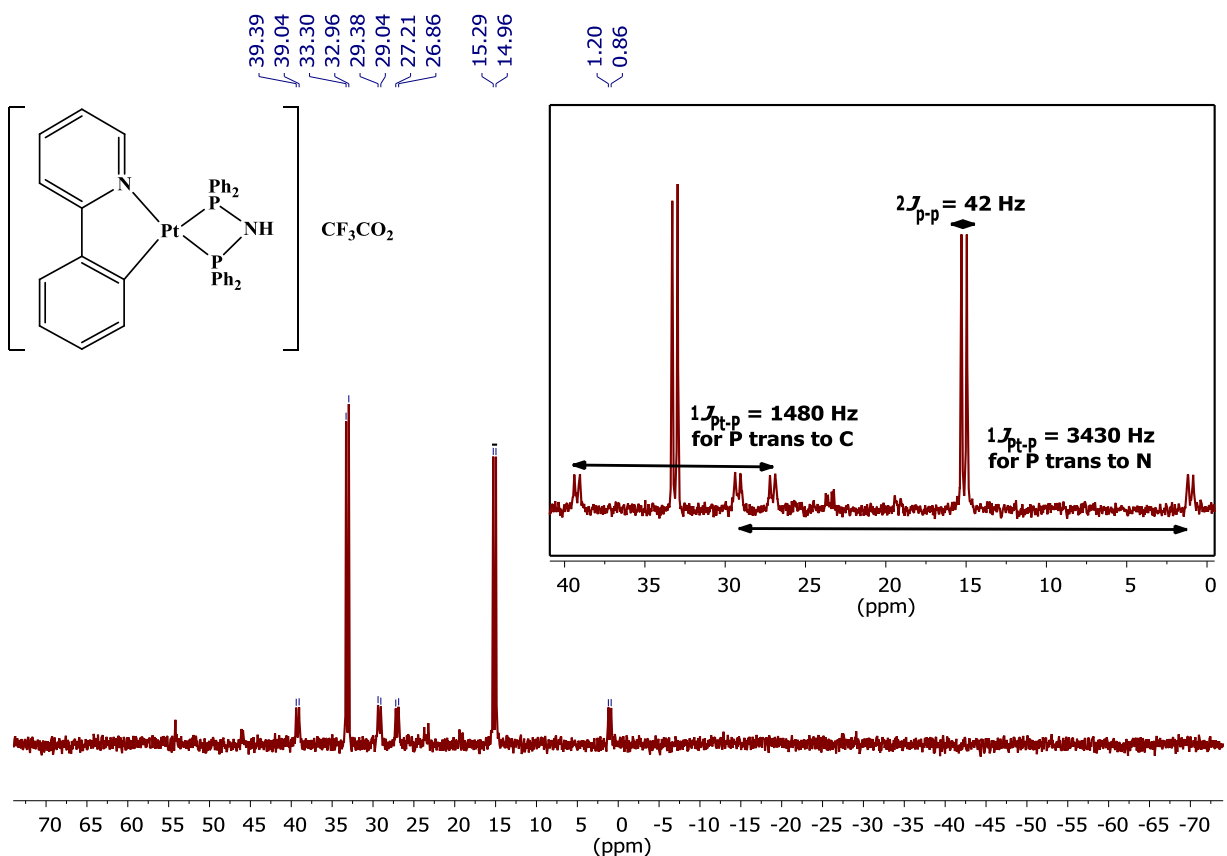


Figure S7. The ^{31}P NMR spectrum of $[\text{Pt}(\text{ppy})(\text{dppa})]\text{CF}_3\text{CO}_2$, **2d**, in CDCl_3 .

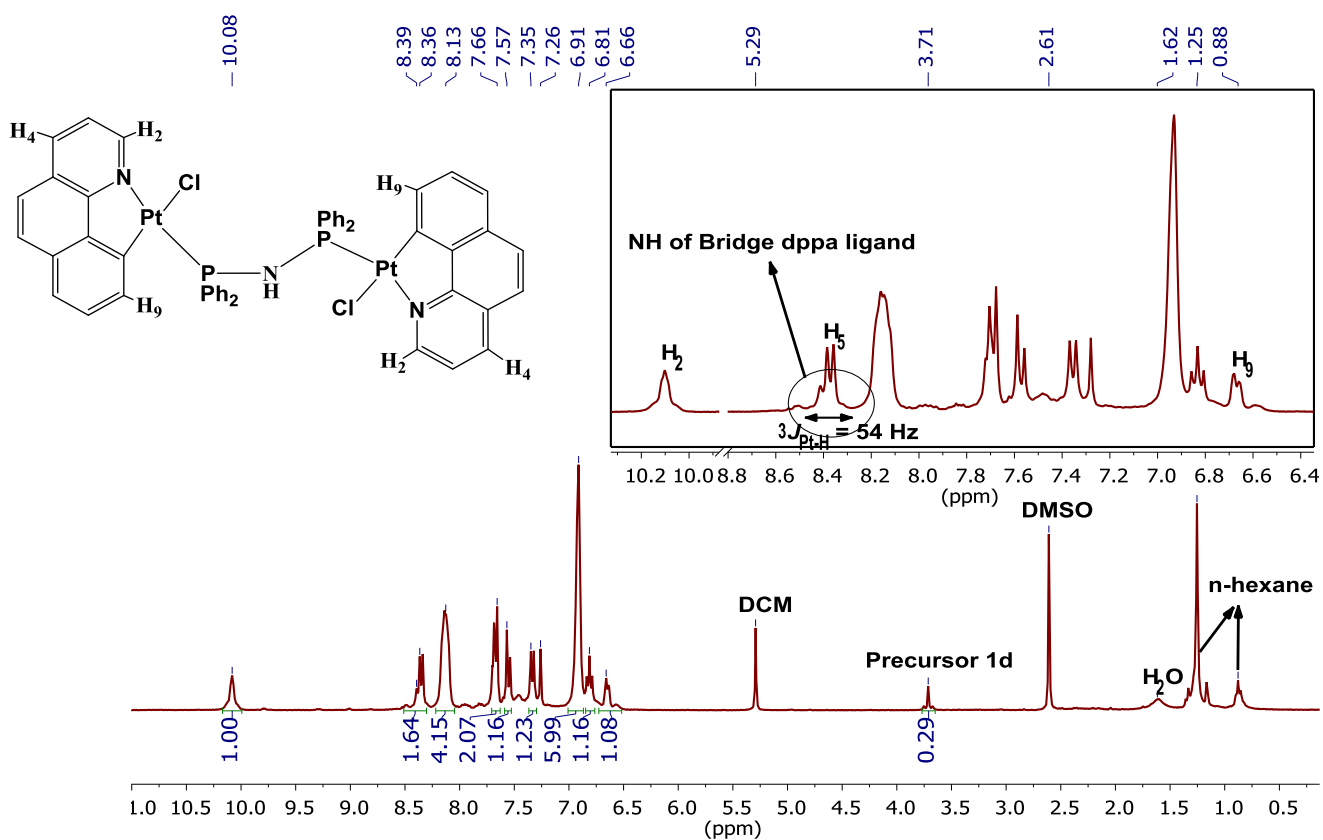


Figure S8. The ^1H NMR spectrum of $[\text{Pt}_2(\text{bhq})_2(\text{Cl})_2(\mu\text{-dppa})]$, **3a**, in CDCl_3 .

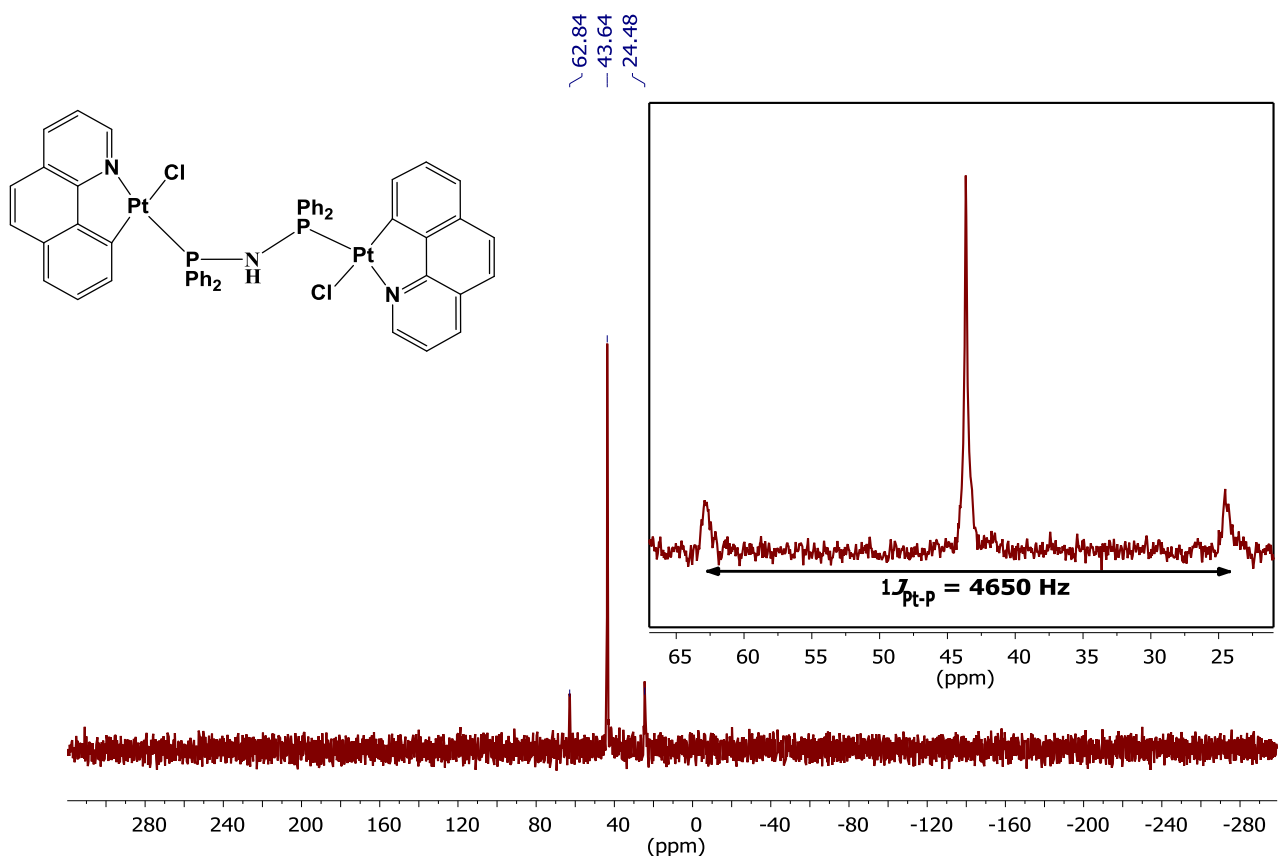


Figure S9. The ^{31}P NMR spectrum of $[\text{Pt}_2(\text{bhp})_2(\text{Cl})_2(\mu\text{-dppa})]$, **3a**, in CDCl_3 .

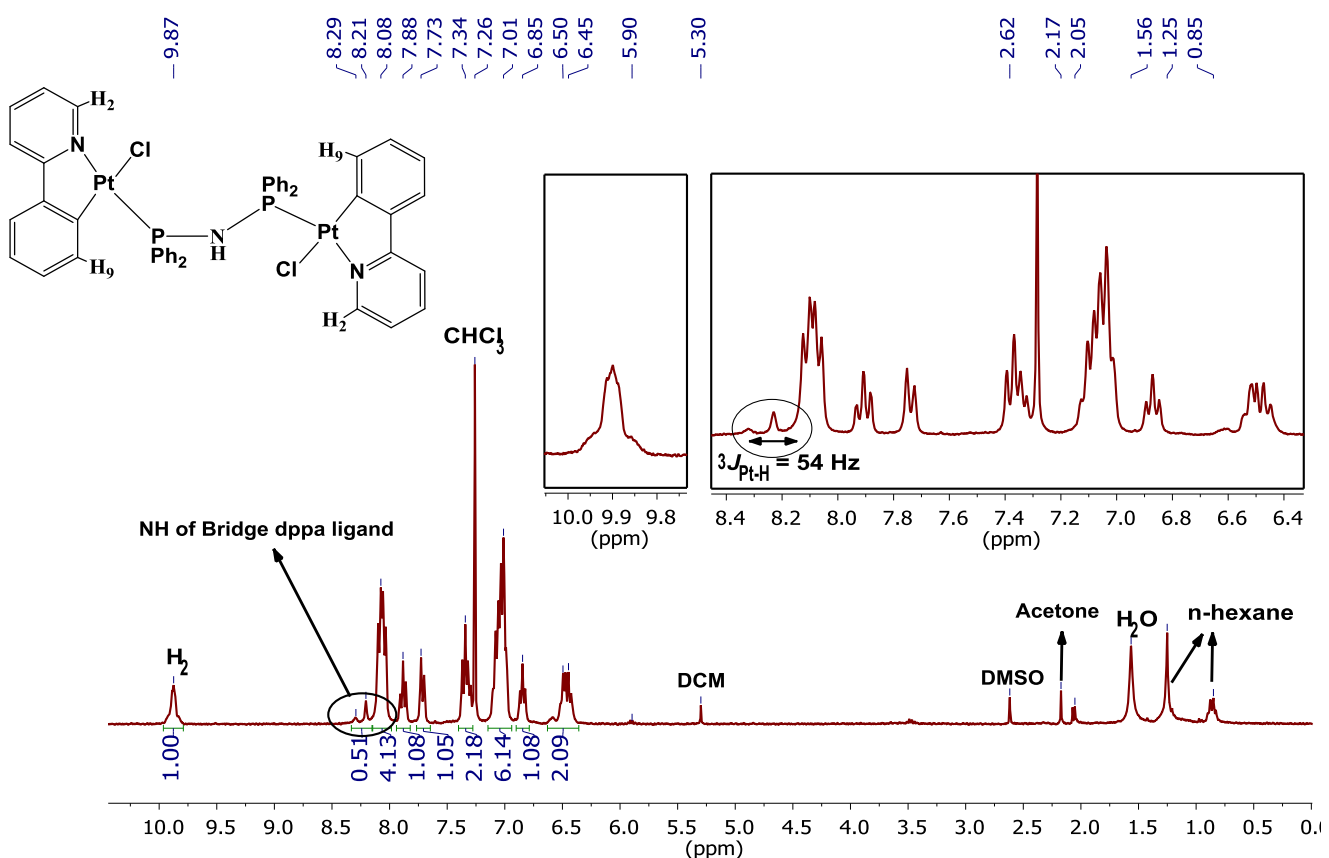


Figure S10. The ^1H NMR spectrum of $[\text{Pt}_2(\text{ppy})_2(\text{Cl})_2(\mu\text{-dppa})]$, **3b**, in CDCl_3 .

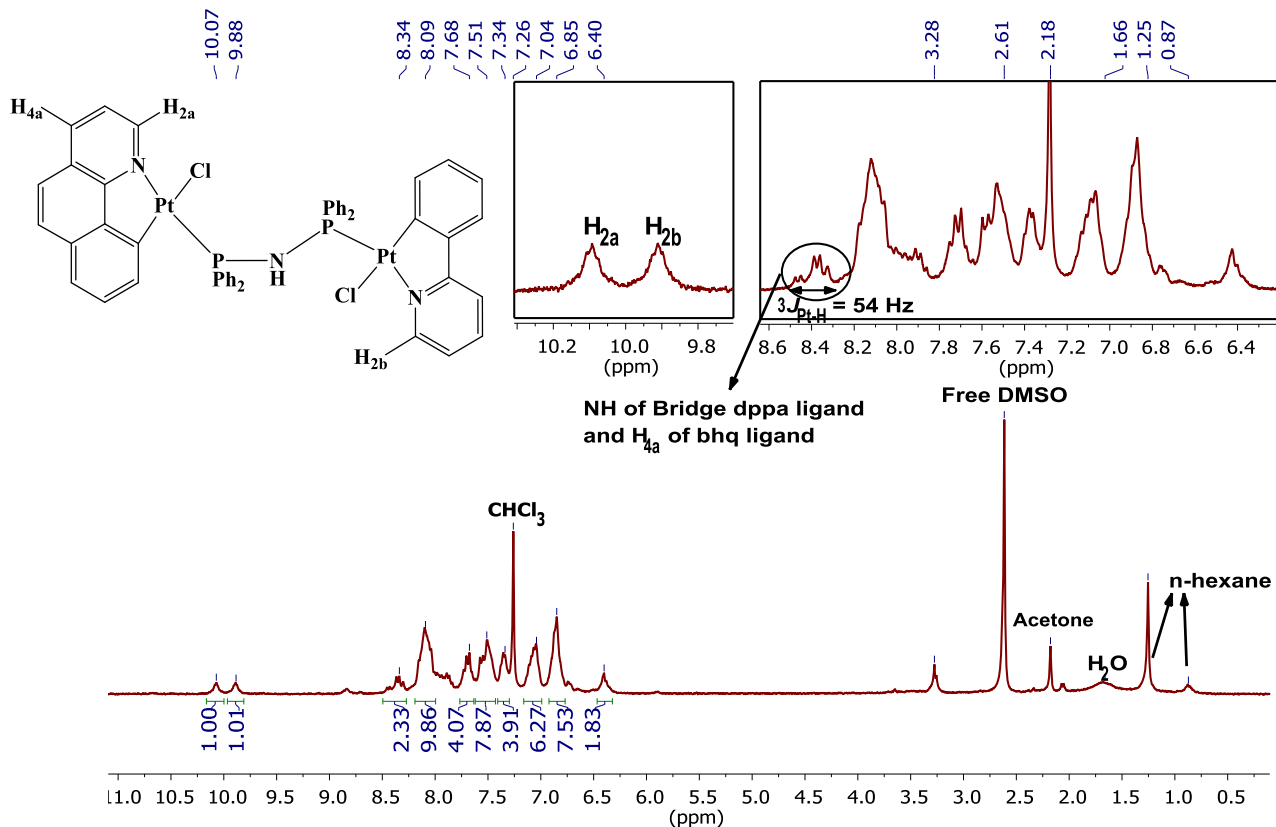


Figure S11. ^1H -NMR spectrum of Unsym-[$\text{Pt}_2(\text{Cl})_2(\text{ppy})(\text{bhq})(\mu\text{-dppa})$], **3c**, in CDCl_3 .

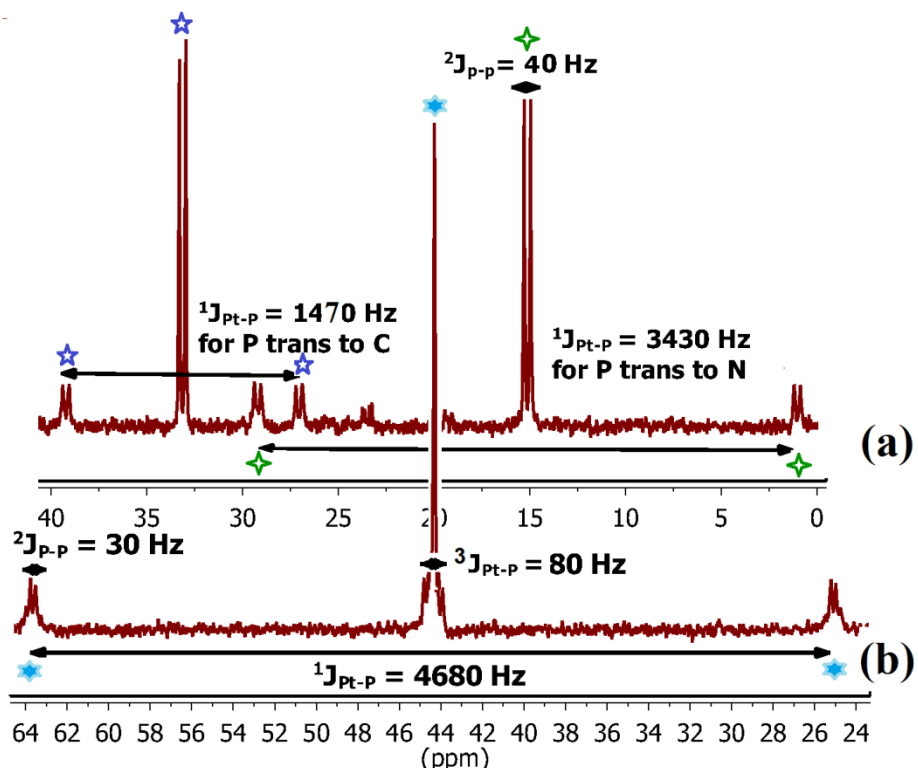


Figure S12. The $^{31}\text{P}\{\text{H}\}$ -NMR spectra of selected complexes: (a) **2b**, and (b) **3b**.

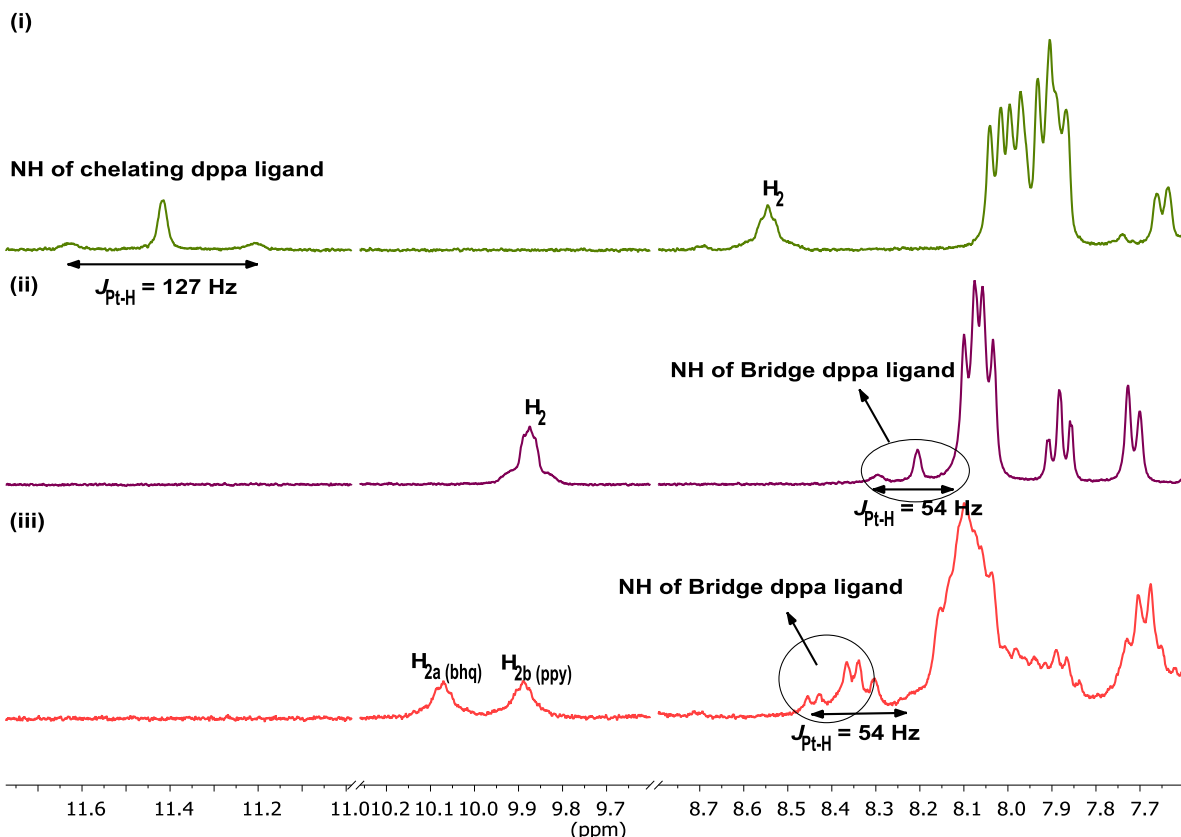


Figure S13. The aromatic region of ^1H -NMR spectra of selected complexes: (i) **2b**, (ii) **3b**, and (iii) **3c**.

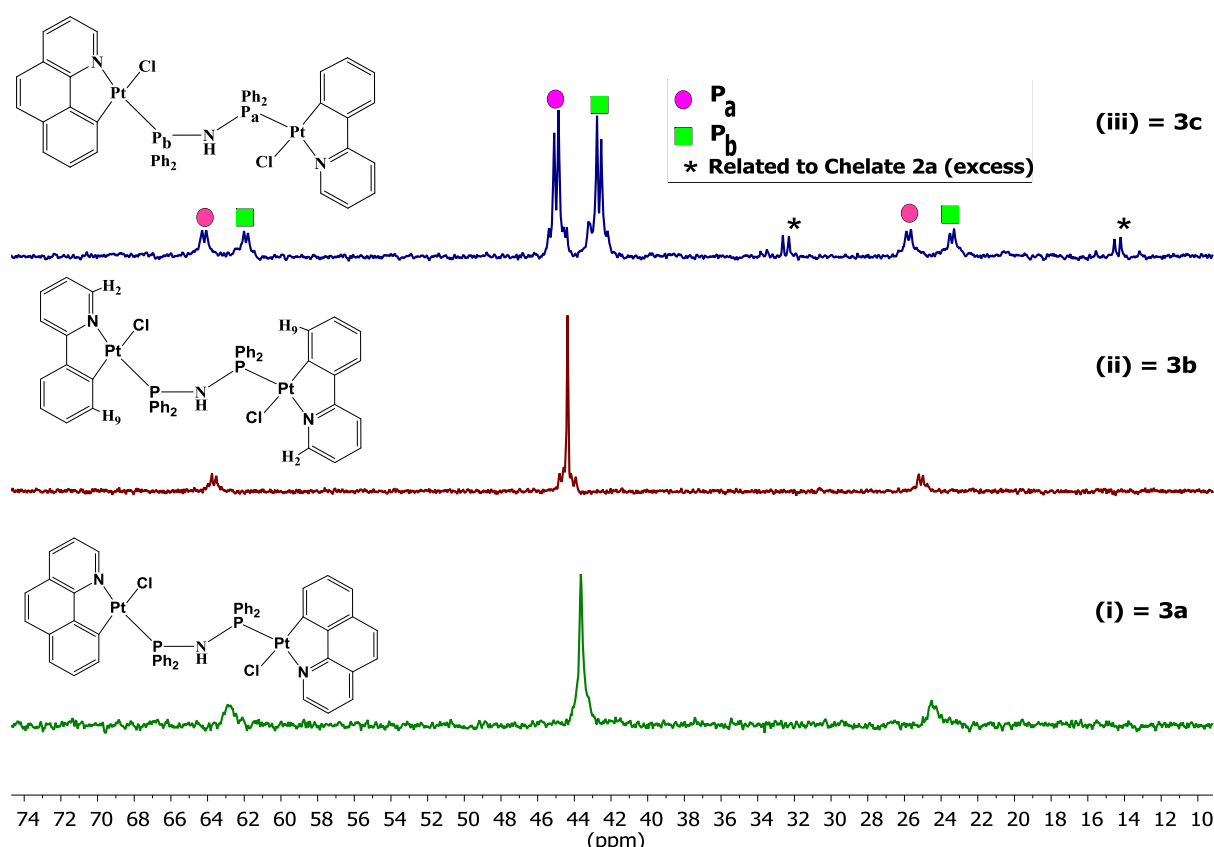


Figure S14. The $^{31}\text{P}\{\text{H}\}$ -NMR spectrum of (i) **3a**, (ii) **3b** and (iii) **3c** in CDCl_3 .

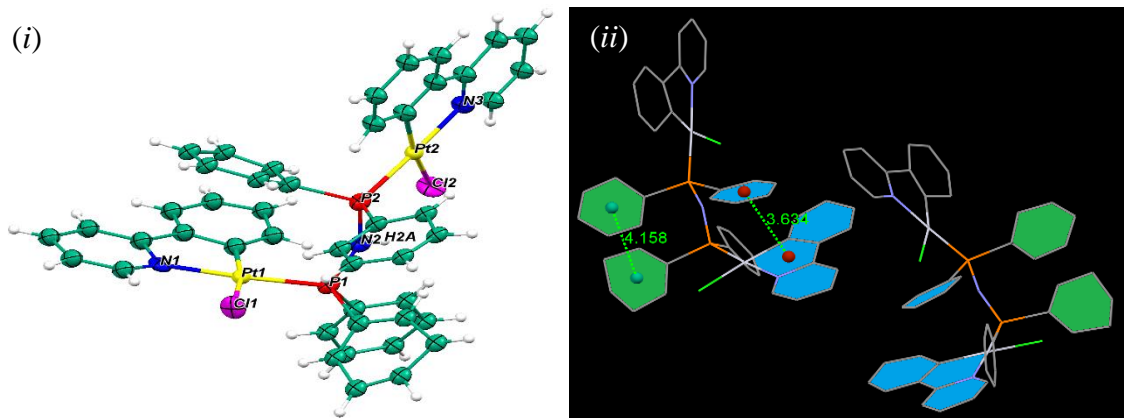


Figure S15. (i) ORTEP representation and (ii) π - π stacking interactions for $[\text{Pt}_2(\text{ppy})_2(\text{Cl})_2(\mu\text{-dppa})]$, **3b**. Ellipsoids are drawn at the 30% probability level, hydrogen atoms are shown as spheres of arbitrary radius. Selected geometrical parameters for **3b** (\AA , $^\circ$): Pt(1)-C(1) 2.00(3), Pt(1)-N(1) 2.08(3), Pt(1)-P(1) 2.221(8), Pt(1)-Cl(1) 2.374(7), Pt(2)-C(36) 1.99(3), Pt(2)-N(3) 2.05(2), Pt(2)-P(2) 2.220(9), Pt(2)-Cl(2) 2.398(6); C(1)-Pt(1)-N(1) 82.4(11), C(1)-Pt(1)-P(1) 95.9(9), N(1)-Pt(1)-P(1) 176.6(7), C(1)-Pt(1)-Cl(1) 170.1(9), N(1)-Pt(1)-Cl(1) 88.1(7), P(1)-Pt(1)-Cl(1) 93.5(3), C(36)-Pt(2)-N(3) 77.5(10), C(36)-Pt(2)-P(2) 98.3(8), N(3)-Pt(2)-P(2) 175.8(6), C(36)-Pt(2)-Cl(2) 167.4(9), N(3)-Pt(2)-Cl(2) 90.8(6), P(2)-Pt(2)-Cl(2) 93.3(3), P(1)-N(2)-P(2) 137.4(14).

Table S1. The crystal data and structure refinement for complexes **2a**, **2c**, **2d**, **3a**, and **3b**.

	2a.H₂O	2c	2d	3a.2CH₂Cl₂.2H₂O	3b
Formula	C ₃₇ H ₃₁ ClN ₂ OP ₂ Pt	C ₃₉ H ₂₉ F ₃ N ₂ O ₂ P ₂ Pt	C ₃₇ H ₂₉ F ₃ N ₂ O ₂ P ₂ Pt	C ₅₂ H ₄₅ Cl ₆ N ₃ O ₂ P ₂ Pt ₂	C ₄₆ H ₃₇ Cl ₂ N ₃ P ₂ Pt ₂
M _t [g mol ⁻¹]	812.12	871.66	847.64	1408.73	1154.79
T [K]	120(2)	120(2)	298(2)	120(2)	298(2)
λ [Å]	0.71073	0.71073	0.71073	0.71073	0.71073
Cryst syst	Monoclinic	Orthorhombic	Monoclinic	Triclinic	Monoclinic
Space group	<i>P</i> 2 ₁ / <i>n</i>	<i>P</i> bca	<i>P</i> 2 ₁ / <i>n</i>	<i>P</i> ī	<i>P</i> 2 ₁ / <i>c</i>
a [Å]	8.9146(18)	17.658(4)	9.2122(18)	10.824(2)	16.840(3)
b [Å]	15.405(3)	17.291(4)	16.750(3)	12.538(3)	13.547(3)
c [Å]	23.179(5)	21.870(4)	22.328(5)	19.399(4)	18.076(4)
α [deg]	90	90	90	108.08(3)	90
β [deg]	95.85(3)	90	99.90(3)	90.42(3)	91.72(3)
γ [deg]	90	90	90	102.08(3)	90
V [Å ³]	3166.6(11)	6677(2)	3394.0(12)	2439.9(10)	4121.7(14)
Z	4	8	4	2	4
ρ [Mg m ⁻³]	1.703	1.734	1.659	1.918	1.861
μ [mm ⁻¹]	4.650	4.355	4.281	6.168	7.025
F(000)	1600	3424	1664	1364	2216
Cryst size (mm)	0.20 x 0.18 x 0.18	0.25 x 0.22 x 0.20	0.50 x 0.50 x 0.45	0.20 x 0.20 x 0.10	0.50 x 0.15 x 0.10
θ range [deg]	2.54 to 25.00	2.49 to 25.00	2.22 to 25.00	1.75 to 25.00	2.22 to 25.00
Limiting indices	-10<=h<=10 -16<=k<=18 -27<=l<=27	-18<=h<=20 -18<=k<=20 -22<=l<=26	-10<=h<=10 -17<=k<=19 -26<=l<=26	-12<=h<=12 -14<=k<=14 -23<=l<=21	-20<=h<=18 -16<=k<=14 -21<=l<=21
Collected Data	14870	19590	15561	18220	18989
Unique Data	5555	5876	5937	8576	7209
R(int)	0.1122	0.1311	0.0990	0.1581	0.2387
Absorption correction	Numerical	Numerical	Numerical	Numerical	Numerical
GOF on F ² [S]	0.0530,0.0836	0.0575,0.0820	0.0536,0.1210	0.0700,0.1055	0.1110,0.2544
R ₁ , wR ₂ [I > 2δ (I)]	0.1070,0.0933	0.1228,0.0945	0.0881,0.1345	0.1592,0.1248	0.1852,0.2785
R ₁ , wR ₂ (all data)					

Table S2. Experimental absorption parameters for complexes **2** and **3** in CH₂Cl₂ and benzene.

	Media ^a	$\lambda_{\text{abs-exp}} / \text{nm} (\epsilon / 10^2 \text{ M}^{-1} \text{cm}^{-1})$
2a	CH ₂ Cl ₂	404 (28.03), 383 (28.03), 347 (31.86), 300 (215.89), 252 (362.21)
	Benzene	410 (5.48), 389 (5.75), 345 (11.56), 302 (39.41), 284 (43.26)
2b	CH ₂ Cl ₂	375 (17.43), 329 (51.46), 273 (238.17), 250 (316.31)
	Benzene	381 (15.81), 330 (62.35), 317 (71.08), 280 (186.56)
2c	CH ₂ Cl ₂	402(28.73), 383(29.83), 345(29.83), 300(220.96), 288(213.35), 256(368.63)
	Benzene	407(17.12), 389(17.48), 349(20.35), 303(118.43), 288(115.56)
2d	CH ₂ Cl ₂	369 (23.35), 330 (63.49), 316 (68.27), 253 (340.74)
	Benzene	375 (20.89), 331 (61.63), 318 (65.17), 280 (202.58)
3a	CH ₂ Cl ₂	406(62.28), 328(159.54), 304(299.97), 261(482.56), 247(460.86)
	Benzene	417(67.04), 399(61.14), 331(161.15), 307(289.50), 269(440.11)
3b	CH ₂ Cl ₂	379(58.03), 328(110.91), 315(127.02), 284(258.11), 250(349.96)
	Benzene	385(55.89), 330(105.85), 319(124.63), 289(236.77)
3c	CH ₂ Cl ₂	386(34.63), 328(85.93), 304(147.86), 258(320.95)
	Benzene	421(19.38), 393(33.59), 330(88.89), 307(138.74), 284(166.43)

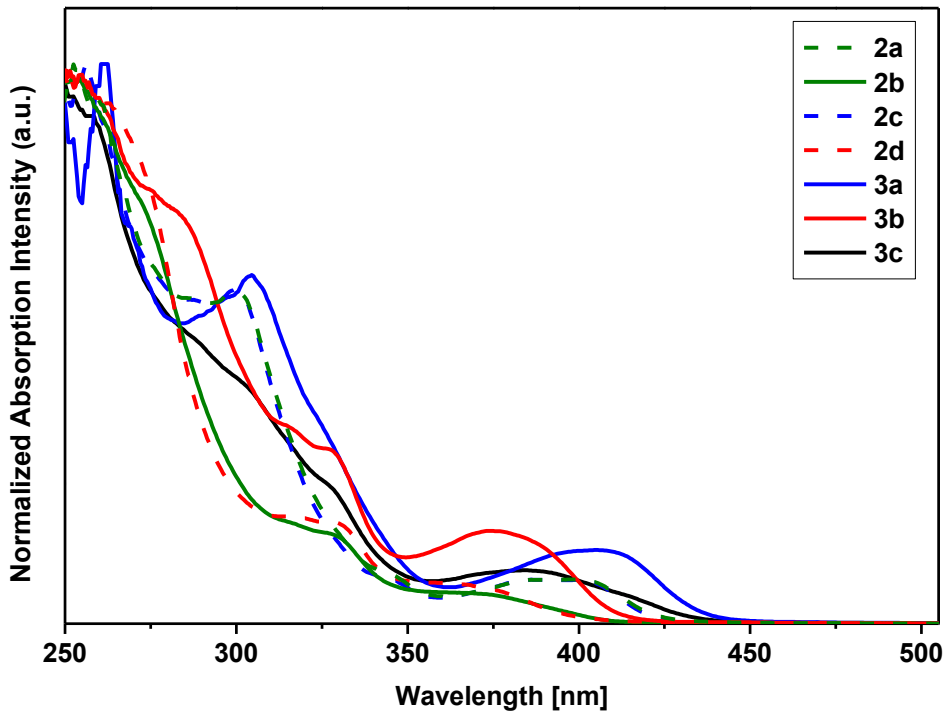


Figure S16. Normalized absorption spectra of complexes **2** and **3** in CH_2Cl_2 at 298 K.

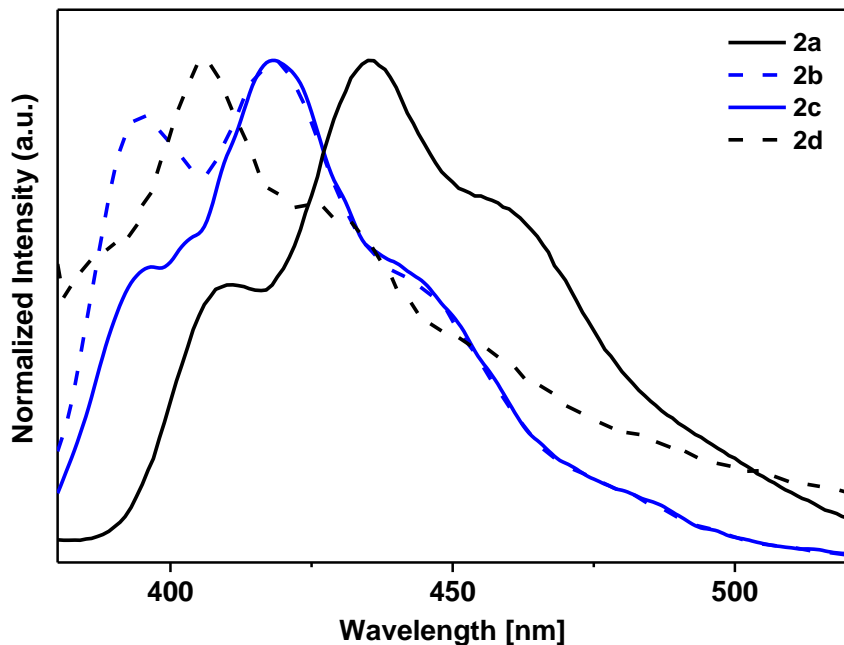


Figure S17. Normalized emission spectra of complexes in CH_2Cl_2 (10^{-4} M) at 298 K.

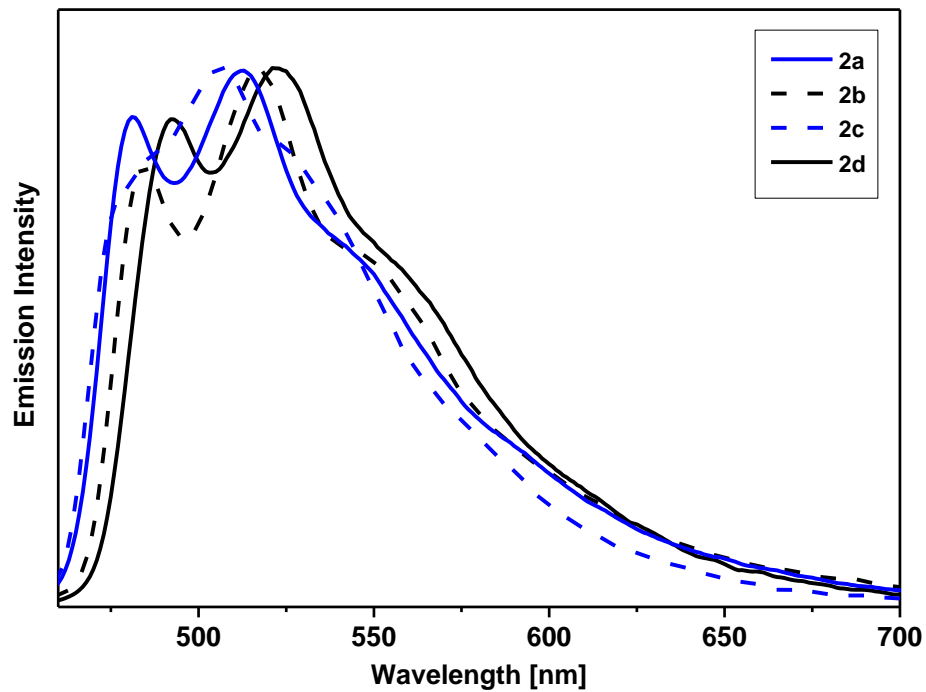


Figure 18. Normalized emission spectra of complexes **2** in powder at 298 K.

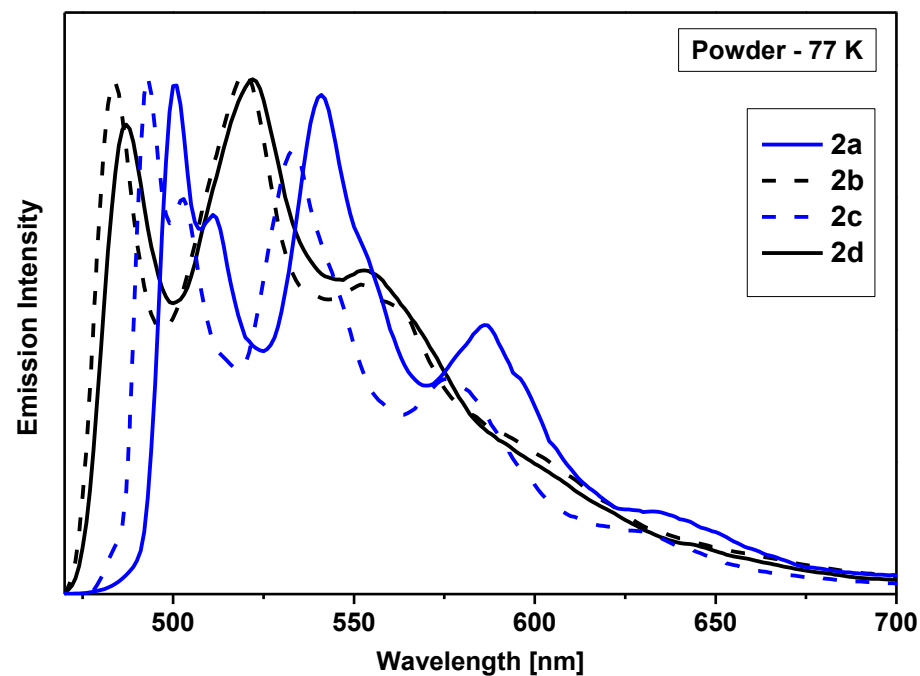
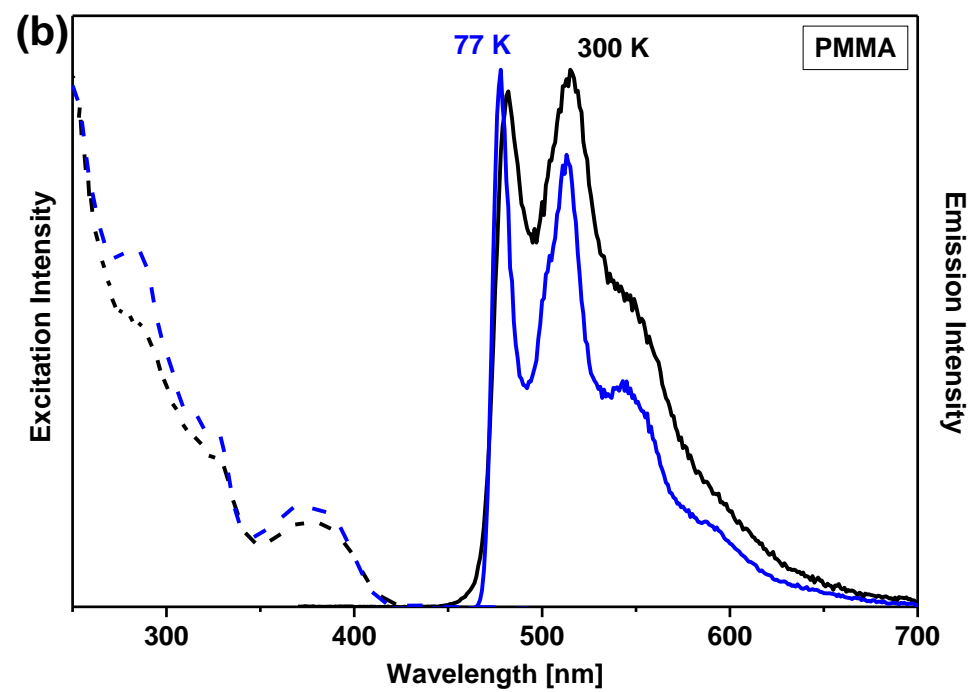
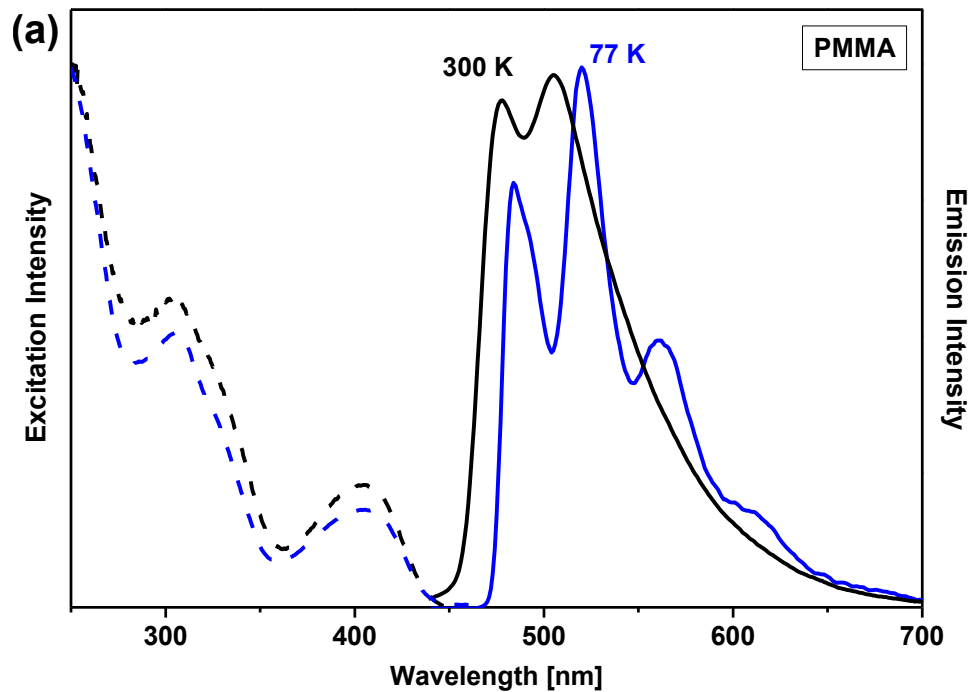


Figure S19. Normalized emission spectra of complexes **2** in powder form at 77 K.



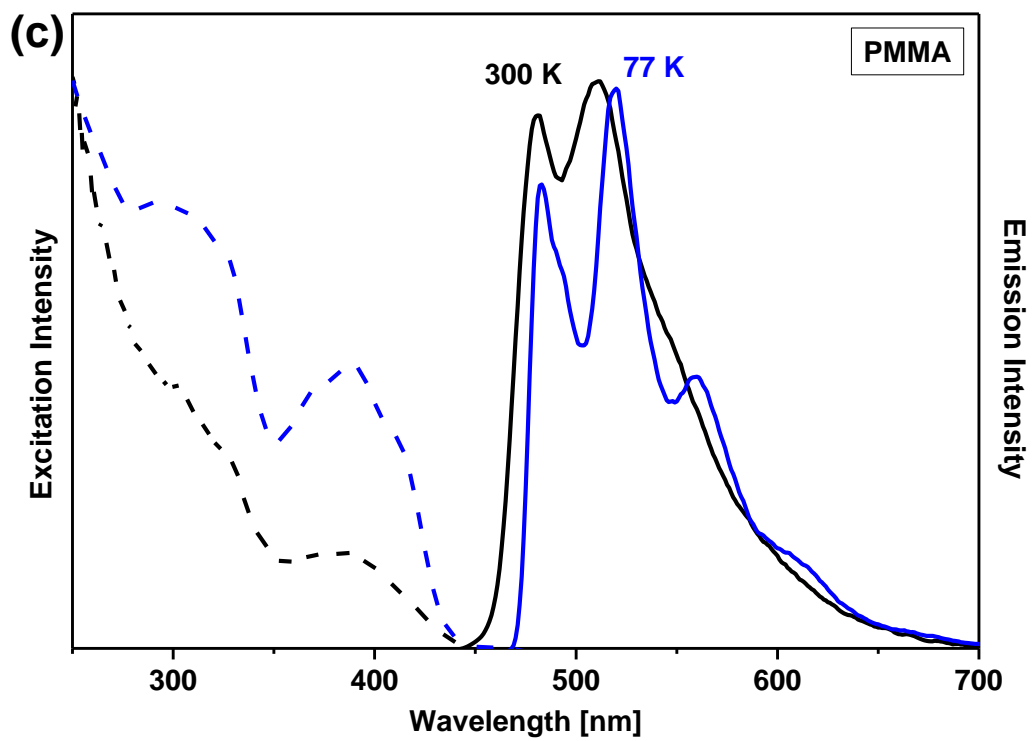


Figure S20. Normalized excitation (dash lines) and emission (solid lines) spectra of (a) **3a**, (b) **3b**, and (c) **3c** in PMMA at 77 K (blue) and 298 K (black).

References:

1. Esmaeilbeig, A.; Samouei, H.; Abedanzadeh, S.; Amirghofran, Z., Synthesis, characterization and antitumor activity study of some cyclometalated organoplatinum (II) complexes containing aromatic N-donor ligands. *J. Organomet. Chem.* **2011**, *696* (20), 3135-3142.
2. Haghghi, M. G.; Nabavizadeh, S. M.; Rashidi, M.; Kubicki, M., Selectivity in metal–carbon bond protonolysis in p-tolyl-(or methyl)-cycloplatinated (II) complexes: kinetics and mechanism of the uncatalyzed isomerization of the resulting Pt (II) products. *Dalton Trans.* **2013**, *42* (37), 13369-13380.
3. M. J. Frisch, G. W. T., H. B. Schlegel, G. E. Scuseria, M. A. Robb, J. R. Cheeseman, G. Scalmani, V. Barone, B. Mennucci, G. A. Petersson, H. Nakatsuji, M. Caricato, X. Li, H. P. Hratchian, A. F. Izmaylov, J. Bloino, G. Zheng, J. L. Sonnenberg, M. Hada, M. Ehara, K. Toyota, R. Fukuda, J. Hasegawa, M. Ishida, T. Nakajima, Y. Honda, O. Kitao, H. Nakai, T. Vreven, J. A. Montgomery, Jr., J. E. Peralta, F. Ogliaro, M. Bearpark, J. J. Heyd, E. Brothers, K. N. Kudin, V. N. Staroverov, T. Keith, R. Kobayashi, J. Normand, K. Raghavachari, A. Rendell, J. C. Burant, S. S. Iyengar, J. Tomasi, M. Cossi, N. Rega, J. M. Millam, M. Klene, J. E. Knox, J. B. Cross, V. Bakken, C. Adamo, J. Jaramillo, R. Gomperts, R. E. Stratmann, O. Yazyev, A. J. Austin, R. Cammi, C. Pomelli, J. W. Ochterski, R. L. Martin, K. Morokuma, V. G. Zakrzewski, G. A. Voth, P. Salvador, J. J. Dannenberg, S. Dapprich, A. D. Daniels, O. Farkas, J. B. Foresman, J. V. Ortiz, J. Cioslowski, D. J. Fox, Gaussian 09, revision D. 01. Gaussian, Inc., Wallingford CT: 2009.
4. Hay, P. J.; Wadt, W. R., Ab initio effective core potentials for molecular calculations. Potentials for the transition metal atoms Sc to Hg *J. Chem. Phys.* **1985**, *82*, 270-283.
5. Cossi, M.; Scalmani, G.; Rega, N.; Barone, V., New developments in the polarizable continuum model for quantum mechanical and classical calculations on molecules in solution. *J. Chem. Phys.* **2002**, *117* (1), 43-54.
6. Barone, V.; Cossi, M.; Tomasi, J., A new definition of cavities for the computation of solvation free energies by the polarizable continuum model. *J. Chem. Phys.* **1997**, *107* (8), 3210-3221.
7. Stoe, C., X-AREA, version 1.30, program for the acquisition and analysis of data. *Stoe & Cie GmbH, Darmstadt, Germany 2005*.
8. Stoe, C., X-RED: program for data reduction and absorption correction, Version 1.28 b. *Stoe & Cie GmbH: Darmstadt, Germany 2005*.
9. Stoe, C., X-SHAPE, version 2.05, program for crystal optimization for numerical absorption correction. *Stoe & Cie GmbH, Darmstadt, Germany 2004*.
10. Sheldrick, G. M., SHELXS-97, Program for crystal structure solution. University of Göttingen, Germany Göttingen: 1997.
11. Sheldrick, G., SHELXL-97: Crystal Structure Refinement Program. *University of Göttingen, Germany 1997*.
12. Prince, E., *International Tables for X-ray Crystallography*. 1995; Vol. C.
13. Stoe, C., X-STEP32, version 1.07 b, crystallographic package. *Stoe & Cie GmbH 2000*.